# Temperature and Frequency Dependence Electrical Properties of $Zn_{1-x}Ca_xO$ Nanoceramic

T. Das, B.K. Das, K. Parashar* and S.K.S. Parashar

Centre for Nanotechnology, School of Applied Sciences, KIIT University, Bhubaneswar-751024, Odisha, India

*(Received March 17, 2016; in final form November 18, 2016)*

This work reports the temperature and frequency dependence electrical properties of Ca doped ZnO ($Zn_{1-x}Ca_xO$, $x = 0.01$) nanoceramic synthesized by solid state reaction method. The X-ray spectra show that the synthesized powder has hexagonal wurtzite structure with space group $P6_3mc$. The average crystallite size decreases with Ca doping. The increase in oxygen positional parameter ($u$) indicates lattice distortion in the crystal structure. Doping with Ca caused a slight shift in the (101) plane peak towards lower diffraction angle. The formation of pores in field emission scanning electron microscopy micrograph may be due to the defect created by Ca substitution. The electrical property was investigated by impedance spectroscopy in the temperature range 300–500 °C. The synthesized sample shows temperature dependence relaxation phenomena and negative temperature coefficient of resistance effects. Electrical conductivity ($\sigma_{ac}$) increases with increase in temperature as well as with frequency due to the drift mobility of electrons and hole by hopping conduction. Dielectric constant was found to decrease with increase in frequency and temperature. This decreases drastically in the magnitude of approximately $<10$ times than the corresponding undoped one.

DOI: 10.12693/APhysPolA.130.1358

PACS/topics: 61.05.cP, 68.37.xy, 84.37.+q, 72.80.Lc, 77.22.Ch

## 1. Introduction

Over the last few years, ZnO has attracted considerable attention due to its many attractive properties, such as the direct wide band gap (3.37 eV), large exciton binding energy (60 meV at room temperature), good piezoelectric characteristics, chemical stability and biocompatibility [1]. It has a stable wurtzite structure with lattice spacing $a = 0.325$ nm and $c = 0.521$ nm and composed of a number of alternating planes with tetrahedrally coordinated $O^{2-}$ and $Zn^{2+}$ ions, stacked alternately along the $c$-axis [2]. Because of its unique properties, low cost and environmental friendly ZnO generated a lot of interest among researchers and technologists for device applications. ZnO has found potential application in different fields, such as gas sensors, solar cells, varistors, light emitting devices, photocatalyst, antibacterial activity, and cancer treatment. ZnO lacks centre of symmetry, which makes it beneficial for its use in actuators and piezoelectric transducers [3].

Properties of ZnO can be tuned by doping metal atoms, to fit specific need and applications. The doping can induce drastic changes in electrical, optical, and magnetic properties of ZnO by altering its electronic structure [4]. In, Ga, and Al doped ZnO improves electrical and optical properties for transparent high power electrical devices. Some other metal like Al, Ta, Cr, La, Ag have been used for better photocatalytic performance [5]. The incorporation of Fe, Co, Ni in the zinc sites of ZnO can result in room temperature ferromagnetism which finds a wide application in spintronics, diluted magnetic semiconductors (DMS), magnetic switches, magnetic sensors, and many more [6]. It has been experimentally and theoretically found that doping of Ca in ZnO is able for blue shift, the band gap modulation and related optical properties were not completely understood [5]. Water and Yang have reported the deposition of Ca doped ZnO thin films by RF sputtering and studied their sensor applications. Mishra et al. found that there is an increase in band width with increase in Ca concentration in ZnO [7]. A number of methods have been devoted for the fabrication of doped ZnO nanoparticles, such as autocombustion method, ball-milling, solid state reaction, coprecipitation, sol–gel process, hydrothermal route, and so on [3]. Among these methods, solid state reaction method is of great interest because of its simplicity and low cost.

However in literature very few reports are available on the electrical properties of Ca doped ZnO nanomaterials. Here we report the result of effect of temperature and frequency on the electrical properties $Zn_{1-x}Ca_xO$ nanoceramic through solid state reaction method for useful technological applications.

## 2. Experimental

Ca doped ZnO ceramic powder abbreviated as $Zn_{1-x}Ca_xO$ ($x = 0.01$) was prepared by using a simple solid state reaction technique. High purity precursor ZnO and $CaCO_3$ were weighted according to their atomic ratio used as a raw material to achieve the desired product. The sample was prepared by thoroughly grinding these powders in an agate mortar and was calcined at 900 °C for 2 h with a heating rate of 2 °C/min using air atmosphere. The calcined powder was mixed with PVA which act as a binder to make pellet. Finally, the pellet

*corresponding author; e-mail: kparasharfch@kiit.ac.in

was sintered at 1000 °C for 2 h in air atmosphere and was coated with silver paste on both sides heated at 700 °C for 15 min. Crystal structure, phase identification and unit cell parameters of $Zn_{1-x}Ca_xO$ ($x = 0.01$) were investigated by using X-ray diffraction (XRD). The surface morphology was observed by field emission scanning electron microscopy (FESEM, Carl Zeiss NTS Ltd, UK). The electrical properties were analysed by using a computer controlled analyzer (Hioki LCR Hi-tester-3532-50) as a function of temperature (30–500 °C) over a wide range of frequency (100 Hz–1 MHz).

## 3. Results and discussion

### *3.1. Structural analysis*

The X-ray patterns of ZnO and Ca doped ZnO ($Zn_{1-x}Ca_xO$, $x = 0$, 0.01) ceramic calcined at 900 °C for 2 h is shown in Fig. 1.

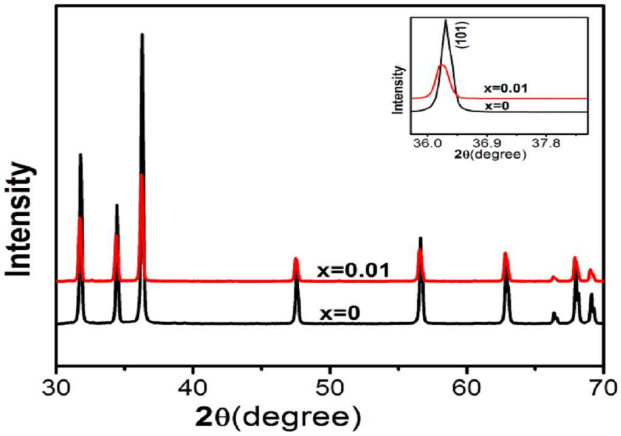


Fig. 1. XRD patterns of $Zn_{1-x}Ca_xO$ ($x = 0$, 0.01) nanoceramic.

It was found that the synthesized powder has hexagonal wurtzite structure with space group of $P6_3mc$ and has a good agreement with JCPDS (data card no: 36-1451). All the peaks were indexed and lattice parameters were calculated by using POWDMULT software as shown in Table I.

TABLE I

Lattice parameters ($a$, $c$ and $c/a$ ratio), $V$ is the volume of unit cell.

| Composition | $a$ [Å] | $c$ [Å] | $c/a$ | $V$ [Å$^3$] |
|---|---|---|---|---|
| $x = 0$ | 3.2488 | 5.2057 | 1.6023 | 47.58 |
| $x = 0.01$ | 3.2521 | 5.2098 | 1.6020 | 47.72 |

It was also observed no identification of secondary peaks confirming single phase and complete solid solubility of $Ca^{2+}$ into ZnO lattice [8]. The change in lattice constant of ZnO is due to higher ionic radius of $Ca^{2+}$ (100 pm) incorporated into smaller ionic radius of $Zn^{2+}$ (74 pm) in their tetrahedral coordinates [9]. The inset of Fig. 1 shows the change in intensity and $2\theta$ along (101) plane. The shifting of (101) X-ray peak towards lower diffraction angle for Ca doped ZnO is clearly shown in the inset figure which provides an indirect evidence that Ca is incorporated into ZnO crystal lattice. The average crystallite size has been estimated by the Scherrer equation [8] and are found to be 50 nm and 34 nm for $x = 0$, 0.01, respectively. Ca doped ZnO has reduced crystallite size and increased peak broadening due to the difference in ionic radii of two ions ($Zn^{2+}$, $Ca^{2+}$) which cause lattice distortion in the crystal structure [10]. The oxygen positional parameter ($u$) calculated for ZnO and Ca doped ZnO are 0.37982 and 0.37988, respectively, by using the relation [11]:

$$u = \frac{1}{3}\frac{a^2}{c^2} + \frac{1}{4}.$$

The bond length (Zn–O) is found to increase with $Ca^{2+}$ substitution which causes a small crystal distortion in crystal structure.

### *3.2. Microstructural analysis*

The surface morphological properties of $Zn_{1-x}Ca_xO$ ($x = 0$, 0.01) nanoceramic was analysed by FESEM. Figure 2 shows the FESEM micrograph of undoped and Ca doped ZnO sintered at 1100 °C for 2 h. This is one

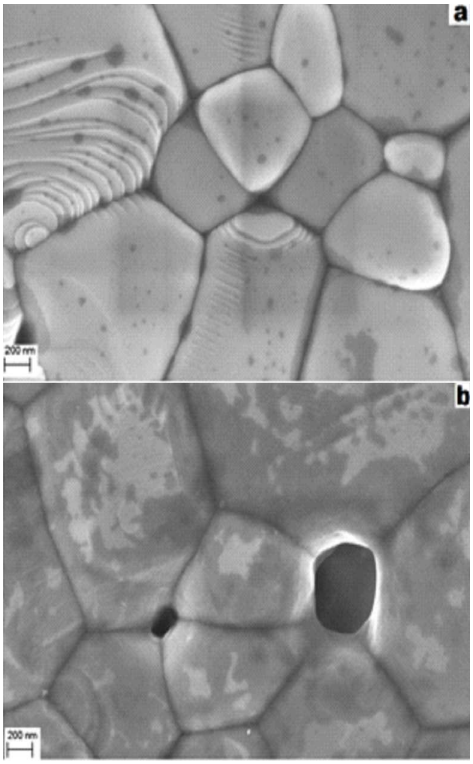


Fig. 2. FESEM micrograph of ZnO (a) and Ca doped ZnO (b) nanoceramic.

of the promising technique used for topography study of the sample and give important information regarding the growth mechanism, shape and size of the particles [8]. The particles are well dispersed in both the samples. The particles of undoped and doped ZnO show good

connectivity, are homogeneous and uniformly distributed over the surface. Ca doped ZnO shows void whereas undoped ZnO shows agglomeration. The formation of void may be due to the defect created by substitution of Ca.

### 3.3. Electrical properties

The variation of dielectric constant ($\varepsilon$) with temperature (30–500 °C) at selected frequency is shown in Fig. 3.

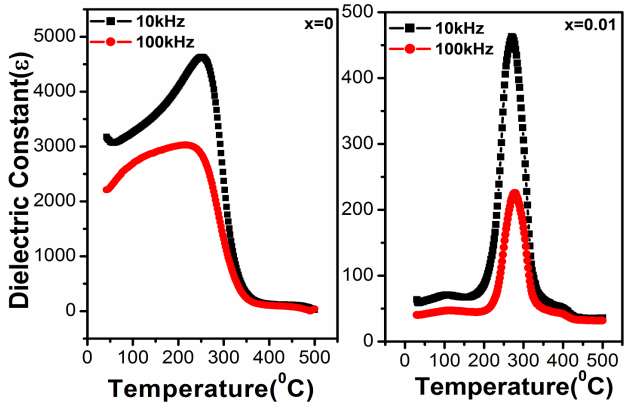


Fig. 3. Variation of dielectric constant for $Zn_{1-x}Ca_xO$ ($x = 0$, 0.01) nanoceramic.

The dielectric constant increases with increase in temperature and reaches a maximum value $\varepsilon_{max}$ at transition temperature ($T_c$) and then decreases with further increase in temperature. It was observed from the figure that the dielectric constant of Ca doped sample is drastically decreased ($\approx$ 10 times) than corresponding undoped one. The narrow peak broadening near $T_c$ and low value of dielectric constant may be due to decrease in crystallite size. Again the value of dielectric constant decreases with increase in frequency. The decrease in dielectric constant at higher frequency can be explained by assuming that solid is composed of well conducting grain separated by poorly conducting grain boundaries. The electron reaches the grain boundary through hopping. If the resistance of grain boundary is high enough, electrons pile up at the grain boundaries and produce polarization. This decreases the probability of electrons reaching the grain boundary and as a result polarization decreases. This in turn decreases the dielectric constant [12].

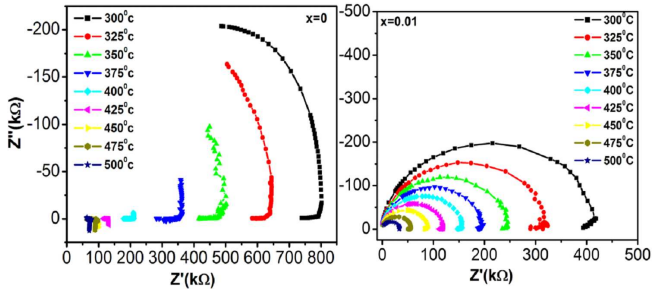


Fig. 4. Cole–Cole plot of $Zn_{1-x}Ca_xO$ ($x = 0$, 0.01) nanoceramic.

Figure 4 shows the Cole–Cole plot of $Zn_{1-x}Ca_xO$ ($x = 0$, 0.01) nanoceramic at different temperature.

It is composed of a high frequency semicircle and a low frequency spike in the temperature. The semicircular pattern in the impedance spectrum indicates the electrical process taking place in the material. This is resulting from the cascading effect of a parallel combination of resistive and capacitance elements arising due to the contribution of the bulk property as well as grain boundary effect [13]. The absence of a third semicircle shows that the electrode–material interface contribution to impedance is very negligible. The semicircular arc decreases gradually with increase in temperature showing the effect of an impedance characteristic of the materials. The impedance spectrum is characterized by the appearance of two semicircular arcs whose centre lies below the real axis. This shows that the non-Debye type of relaxation obeys the Cole–Cole formalism. This behaviour is correlated with several factors such as grain size distribution, grain orientation, grain boundaries, etc. It was observed from Fig. 4 that ZnO ($x = 0$) does not have any clear semicircular arc at different temperatures. The semicircular arcs are generated only at temperature interval between 300 and 375 °C showing major contribution of grain boundary resistant. Ca doped ZnO has semicircular arcs indicating the contribution from both grain boundary and grain resistance. It clearly shows that the material is temperature and frequency dependent.

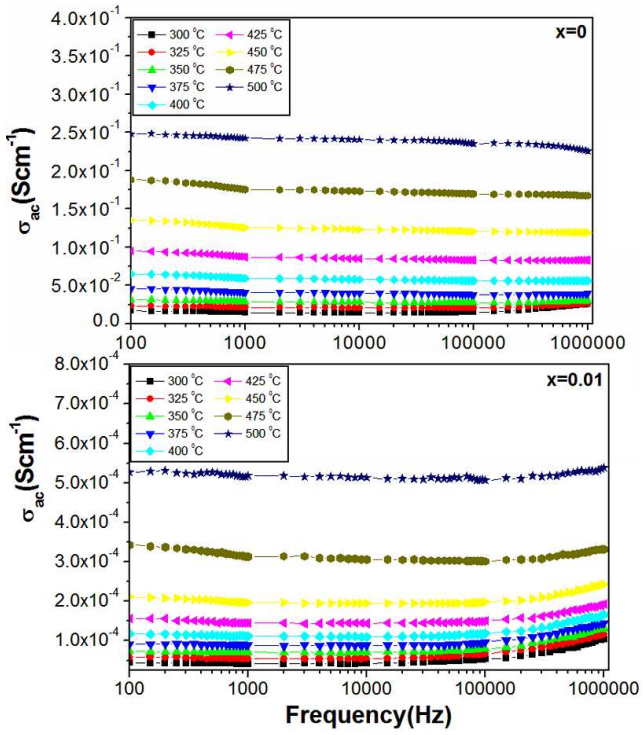


Fig. 5. Frequency dependence ac conductivity of $Zn_{1-x}Ca_xO$ ($x = 0$, 0.01) nanoceramic.

The frequency dependence ac conductivity of $Zn_{1-x}Ca_xO$ ($x = 0$, 0.01) nanoceramic as a function of

temperature is shown in Fig. 5. Electrical conductivity ($\sigma_{ac}$) as evaluated from complex impedance spectrum in the synthesized sample is due to the hopping of electrons. Here study of ac conductivity is carried out to understand the frequency dependence of electrical properties of the material and to get information regarding the nature of charge carriers. Beside that conductivity analysis provide significant information related to transport to charge carrier. It was observed from the figure that the ac conductivity increases for all samples with increase in temperature which indicates the electrical conduction in the material. The conductivity also increases with increase in frequency showing semiconducting behaviour. The increase of electrical conductivity with increase in temperature and frequency may be related to increase of the drift mobility of the electron and hole by hopping conduction [14]. The total conductivity of the system is given by [15]:

$$\sigma_{\text{tot}} = \sigma_0\,(T) + \sigma(\omega T).$$

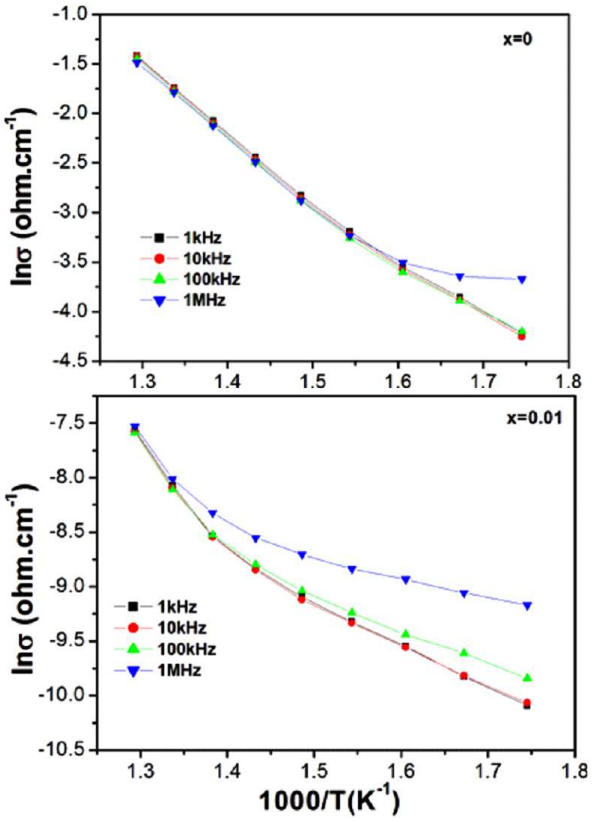


Fig. 6. Electrical conductivity versus inverse of temperature for $Zn_{1-x}Ca_xO$ ($x = 0$, 0.01) nanoceramic.

Here the first term on right hand side is dc conductivity due to band conduction which is independent of frequency. The second term is pure ac conductivity due to the hopping of charge carrier between the metal ions. The conductivity decreases with Ca doping which may be due to introduction of defect created by $Ca^{2+}$ ion in ZnO system. The increase in conductivity with respect to temperature indicates the negative temperature coefficient of resistance (NTCR). With increase in temperature (Fig. 6), the conductivity was found to increase in both cases which can be attributed to the free as well as bound carriers from different region in ceramics such as grain and grain boundaries that are distributed non-homogeneously and this leads to a change in activation energy with temperature. These charge carriers may arise from dopant Ca ions or oxygen vacancies [16–18].

The activation energy ($E_a$) at 10 kHz of the synthesized sample was calculated by using the Arrhenius equation and was found to 0.29 eV and 0.36 eV for $x = 0$ and $x = 0.01$, respectively. The increase in activation energy confirms the increase in barrier energy for electron hopping.

## 4. Conclusions

$Zn_{1-x}Ca_xO$ ($x = 0$, 0.01) nanoceramics have been successfully synthesized by solid state reaction method. The average crystallite size decreases with Ca doping. The increase in oxygen positional parameter ($u$) indicates lattice distortion in the crystal structure. The dielectric constant near the phase transition temperature for Ca doped ZnO decreases sharply in comparison to undoped ZnO. The formation of pores in FESEM micrograph of Ca doped ZnO may be due to the defect created by Ca. The experimental results indicate that dielectric properties, impedance and ac conductivity decrease with increase in temperature and frequency. These results are an indication that Ca doped ZnO nanoceramic may be useful for electrical applications.

## References

[1] S. Maensiri, C. Masingboon, V. Promarak, S. Seraphin, *Opt. Mater.* **29**, 1700 (2007).

[2] B.K. Das, T. Das, K. Parashar, S.K.S. Parashar, *Appl. Sci. Adv. Mater. Int.* **1**, 17 (2014).

[3] S. Singhal, J. Kaur, T. Namgyal, R. Sharma, *Physica B* **407**, 1223 (2012).

[4] Y. Liu, J. Wang, C. Xu, Z. Si, S. Xu, S. Shi, *J. Mater. Sci. Technol.* **30**, 860 (2014).

[5] D. Li, J.F. Huang, L.Y. Cao, J.Y. Li, O. Yang, C.Y. Yao, *Ceram. Int.* **40**, 2647 (2014).

[6] N.R. Yogamalar, A. Chandra Bose, *Prog. Nanotech. Nanomater.* **2**, 1 (2013).

[7] R. Udayabhaskar, R.V. Mangalaraja, B. Karthikeyan, *J. Mater. Sci. Mater. Electron.* **24**, 3183 (2013).

[8] S. Muthukumaran, R. Gopalkrishnan, *Opt. Mater.* **34**, 1946 (2012).

[9] S.B. Rana, P. Singh, A.K. Sharma, A.W. Carbonari, R. Dogra, *J. Optoelectron. Adv. Mater.* **12**, 257 (2010).

[10] P. Kumar, Y. Kumar, H.K. Malik, S. Annapoorni, S. Gautam, K. Hwa Chae, K. Asokan, *Appl. Phys. A* **114**, 453 (2013).

[11] U. Ozgur, Ya.I. Alivov, C. Liu, A. Teke, M.A. Reshchikov, S. Dogan, V. Avrutin, S.J. Cho, H. Morkoç, *J. Appl. Phys.* **98**, 041301 (2005).

[12] C. Venkataraju, G. Sathishkumar, K. Sivakumar, *J. Alloys Comp.* **498**, 203 (2010).

[13] S. Sen, P. Pramanik, R.N.P. Choudhury, *Appl. Phys. A* **82**, 549 (2006).

[14] F.S.H. Abu-Samaha, M.I.M. Ismail, *Mater. Sci. Semicond. Process* **19**, 50 (2014).

[15] A.M. Abo El Ata, M.K. El Nimra, S.M. Attia, D. El Kony, A.H. Al-Hammadi, *J. Magn. Magn. Mater.* **297**, 33 (2006).

[16] S.K.S. Parashar, B.S. Murty, S. Repp, S. Weber, E. Erdem, *J. Appl. Phys.* **111**, 113712 (2012).

[17] E. Erdem, *J. Alloys Comp.* **605**, 34 (2014).

[18] H. Kaftelen, K. Ocakoglu, R. Thomann, S. Tu, S. Weber, E. Erdem, *Phys. Rev. B* **86**, 014113 (2012).